Modular Static Distribution Controller for Distributed Energy Resource Generation Applications

Faris E. Alfaris
Student member, IEEE
Electrical and Computer Engineering
North Carolina State University
Raleigh, United States
Fealfari@ncsu.edu

Nima Yousefpoor
Member, IEEE
Quanta Technology
Raleigh, United States
nyousefpoor@quanta-technology.con

Subhashish Bhattacharya
Senior member, IEEE
Electrical and Computer Engineering
North Carolina State University
Raleigh, United States
Sbhatta4@ncsu.edu

***Abstract* -- Recently, renewable wind generations (WG) is enjoying a rapid growth globally amongst other renewable energy sources due to their lower cost and technology advancement. However, the intermittent nature of wind energy and performance of the attached induction generators inevitably poses some challenges to the power grid integrated large-scale wind-farms (WF), especially in case of weak power system. These challenges include frequency oscillations, voltage variation and power quality issues. To overcome these problems and facilitate the WF integration, this study proposes a modular static distribution controller (MSDC) at the WF point of interconnection (POI). The MSDC is composed of a dc-ac power converter connected to a dc/dc chopper converter and energy storage system. The overall power electronic system is considered as a versatile controller which is connected at the POI of WFs, and it can perform several tasks including frequency regulation, reactive power support, voltage control, harmonic filtering, power smoothing, and dynamic load balancing. The detailed model of the MSDC is presented and its control system is developed. In this paper, the dynamic performance of MSDC system is evaluated to achieve different objectives, and the operation of MSDC is validated in an actual weak power system under different modes of operation.**

***Index Terms*— Accommodation of renewable resources, distributed generation controller, energy storage system, facilitating development for distributed electricity generations, integration of distributed generations, power quality improving.**

I. INTRODUCTION

The steep growth of renewable energy resources, due to the rapid technology advancement, raised the concerns about the power stability and power quality issues caused by the penetration and fluctuation in the generated power [1-2]. Most specifically, the wind generation (WG) inevitably causes a wide range of issues on a transmission and distribution systems such as: frequency oscillations, power and voltage fluctuation. These problems are caused by the variation of wind speed in a short and medium time intervals [3-4]. Figure 1 shows the WG growth over the last fifteen years. Due to the fact that utilities are strict about criteria and requirements, therefore, the power system developers must meet these requirements before authorizing interconnection of large scale wind farms (WF) to distribution feeders. These requirements includes:

a) Power factor requirement: Generally, as required by most Large Generator Interconnection Agreement (LGIA), all generation resources 20 MVA and above must be able to deliver to the Point of Interconnection (POI) reactive power output equivalent to a 0.95 power factor calculated at the generation resource's maximum net power [5].
b) Harmonic requirement: The WG system can have fairly consistent harmonic current mission characteristics over time depending on the individual wind turbines characteristics and the partial use of electric power converters. IEEE-519 recommends the harmonic distortion limits intended for application at POI, and the harmonic requirement should be met at the POI of WG system according to IEEE-519 standard.
c) Flicker requirement: The WG system is characterized by repeated or sudden power fluctuations which can produce rapid voltage changes on the supply system to which it is connected. IEEE-1453 recommends the flicker limits intended for application at POI.
d) Temporary overvoltage (TOV) requirement: IEEE-1547 recommends the TOV limits due to unbalanced operating conditions including islanding and single line to ground fault.
e) Online frequency requirement: The sudden change in the grid loads or power supplied by main power generators and WFs causes deviation or fluctuation in the grid frequency. These frequency dynamics, including rate of change of frequency (ROCOF), are partially dominated by the kinetic energy stored in the power plant generators. However, the frequency dynamic issues become more significant in case of weak power grid or lower system inertia due to the increase using of renewable sources (Fig. 2), hence, a faster transient frequency support unit is needed [6-7].

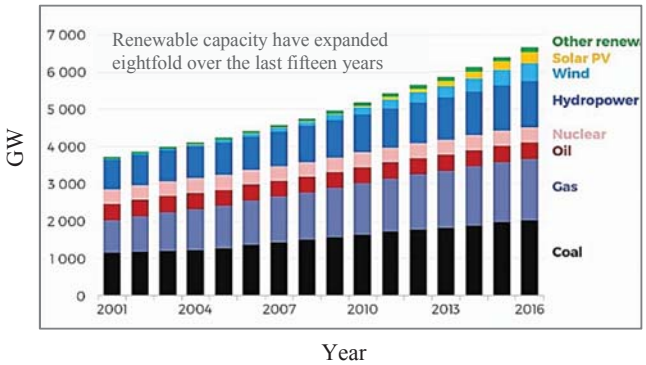

Fig. 1. Annual growth of the global renewable energy capacity since 2000 [8].

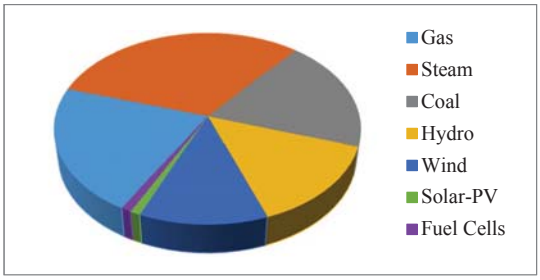

Fig. 2. Average inertia constant for different generation turbines [7].

Based on the aforementioned, a Modular Static Distribution Controller (MSDC) is proposed in this study as a versatile device to significantly enhance the injected power quality and system dynamic performance in order to meet the technical specifications required by grid codes.

The dynamic performance of the MSDC device with its controller functionalities when used in an actual weak power system is evaluated under different modes of operation. The power system is provided by Bonneville Power Administration (BPA) and described in the next section. The detailed model of the power system, generated power, actual wind farms data and consumed power were simulated, and the impact of the feasible solution is studied using PSCAD/EMTDC simulation environment. The field data, collected by supervisory control and data acquisition (SCADA), were used in the simulation process in order to obtain the capability of the MSDC to achieve the desired targets in reality. The lab scale experimental testbed for MSDC is planned for future work, to investigate the different aspects in the hardware implementation of the MSDC.

II. System Configuration

The single line diagram of the 12-bus power system, analyzed in this study, is shown in Fig. 3. The system consists of three power generators and two large-scale WFs at buses #4 and #10. Bus #1 considered to be the slack bus where the voltage and power angle are known. The system is in closed loop configuration to improve the reliability of power supply. The power and voltage ratings of WF1 and WF2 are 100 MVA/115 kV and 50 MVA/34.5 kV; respectively. WF1 includes variable speed doubly fed induction generators (DFIGs) with partial use of back-to-back (BTB) converters. The BTB converters are utilized to compensate the reactive power at bus #4 in order to regulate the bus voltage. The lower rating wind farm WF2 uses a fixed speed squirrel-cage induction generators (SCIGs), and it is connected to the 69 kV loop system. In addition, WF2 turbines are not facilitated with wind speed controller which poses the challenge of unsettled voltage and frequency at bus #10. Therefore, the sub-transmission system that linked WF2 to the power grid is considered as the weakest part of the loop system. In [2] and [9], it is shown that connecting the weak portion of a system with an oscillatory power source causes several significant problems such as power stability and power quality issues that limits the amount of injected power.

Moreover, the loads located nearby the weak sub-transmission and sensitive to voltage variation, (e.g. induction motors), are exposed to harm or damage [10]. To solve this problem, low-cost mechanical switched capacitors in range of hundred kilovars are installed across bus #10, and the main power transformers are equipped with tap-changing (TC) setting to provide voltage support at the connected buses. However, due to the stepped and slow response of these devices, the aforementioned dynamic issues cannot be satisfactorily redeemed, and even they might get aggravated.

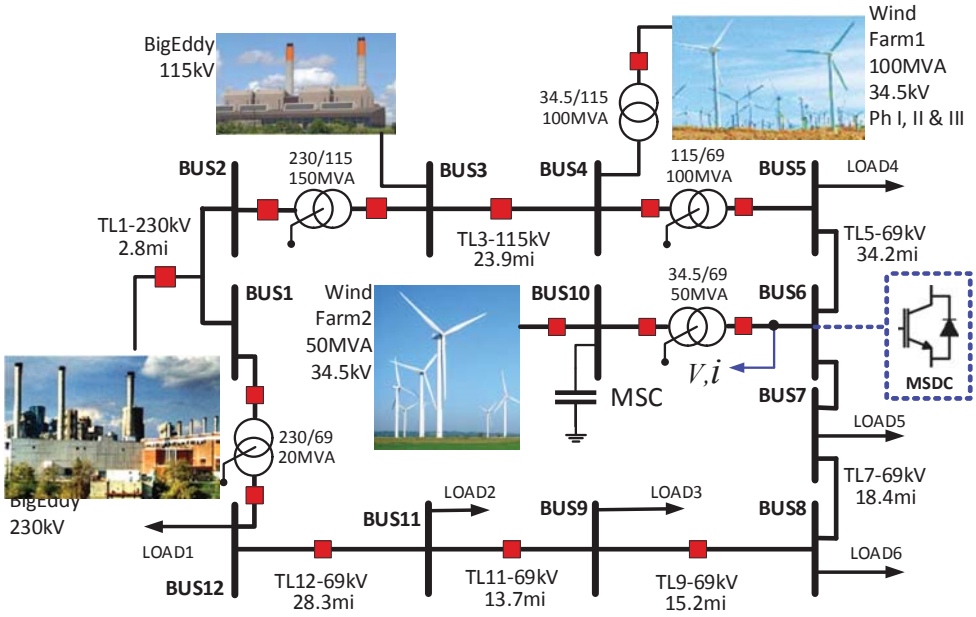

Fig. 3. Single line diagram of the BPA system.

III. MODULAR STATIC DISTRIBUTION CONTROLLER

A. Operation Principle and Dynamic Model

The MSDC is a versatile distribution controller which can be connected at a medium voltage bus to perform several tasks in different operation modes as follows: Mode 1) Reactive power support to meet utility power factor requirement, Mode 2) Voltage support to meet utility flicker requirement, Mode 3) Act as an active filter to mitigate harmonic distortions at POI to meet utility harmonic requirement and Mode 4) Act as a dynamic balancing device to improve grid stability, seamless mode transitions, and minimize load interruptions.

The MSDC consists mainly of a fast-response energy storage system (ESS), bi-directional DC-DC chopper converter, DC-link capacitor and DC-AC converter as illustrated in Fig. 4. The DC-AC converter is required to condition the decoupled active and reactive power in order to achieve the desired functions, whereas the boost converter is used to adapt different levels of DC voltage by directing the electric power either to charge or discharge the ESS, based on the nature of the injected power. Controlling the DC link voltage via the boost converter, instead of the DC-AC converter, assures its sustainability where the power dc-ac converter interfaces a weak power grid.

The DC-AC converter employs a step-up delta-wye transformer to meet the grid voltage level and isolate the zero-order harmonics. The DC-DC converter acts as a boost converter when the real power direction is from ESS to the grid, and acts as a buck converter during the opposite power direction. Different modular power converter topologies will be explored and compared in future work to find the most appropriate voltage source converter topology for the application of MSDC.

The detailed model of the DC-DC converter is shown in Fig. 5. The design of this converter takes into account the continuity and small ripple of the ESS current in order to reduce the input current harmonics, and therefore the ESS power losses. To this aim, the DC converter input inductor is optimally designed to operate under continuous conduction mode (CCM), with 350 *ms* maximum response time constant and 2% maximum ripple of the ESS input current for all possible operations.

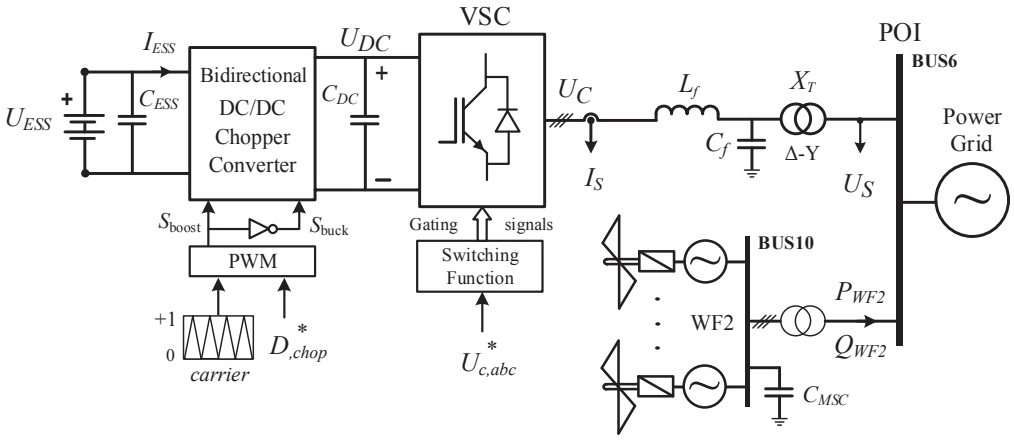

Fig. 4. The general configuration of the MSDC system connected at the POI bus.

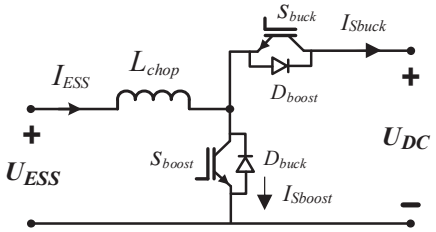

Fig. 5. Detailed model of the DC-DC chopper converter.

B. Converters Design Considerations

The MSDC is a transportable modular conversion unit and it is potentially a cost effective device since it utilizes the standard power electronics converter systems, for instance, standard medium voltage drive converters. The key component of the DC-AC converter is semiconductor switches and circuit topology, and better performance can be obtained through hybrid semiconductor configuration (like Si switch and SiC diode). Currently, standard medium voltage drive systems are commercially available up to 10 MVA with IGCT based three-level NPC converters and up to 2 MVA with IGBTs which are more than 97% energy efficient.

With advent of new high voltage SiC based semiconductor switches such as 15kV SiC IGBT and 10kV SiC JBS diode technologies higher power and higher efficiencies can be foreseen for MSDC building blocks. Different power converter topologies including Cascaded H-bridge converter and Modular Multilevel Converter (MMC) for the use in Battery Energy Storage System (BESS) applications, as discussed in [11], will be investigated and compared in the future work to be utilized optimally as a basic building block for the MSDC.

IV. CONTROL SYSTEM

The MSDC is controlled by employing two subsystems; DC-DC control system and DC-AC control system.

A. DC-DC control system

The schematic diagram of the DC-DC converter controller, used to interface the ESS to the VSC, is shown in Fig. 6. The current-mode control, also called current programmed mode, is utilized where the voltage and current control loops are existed. This technique provides a direct control to the peak inductor current or shunt switch current I_{Sboost}, instead of DC voltage, to enhance the converter dynamics [12-13]. The squared DC voltage reference is used in sake of better operation stability based on Lyapunov's energy function [13].

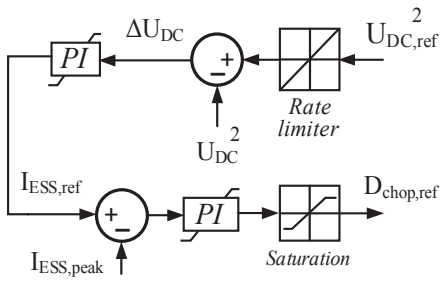

Fig. 6. Control circuit of DC-DC chopper converter.

B. DC-AC control system

The controller circuit of the DC-AC converter is divided into three parts: supervisory control loop, inner control loop, and synchronization module. The objective of the supervisory control loop is to determine the reference values of active and reactive power flow, by adjusting, respectively, the *d*-axis and *q*-axis components of the converter current, according to the mode of operation. The objective of the inner control loop is to track the generated reference signals by controlling the converter output currents. The synchronization module is used to transform the measured signals from *abc* reference frame to *d-q* reference frame and track the system angular speed using a phase-locked-loop (PLL). Fig. 9 shows the schematic of the control diagram in *d-q* reference frame.

B.1 Reference Signals Formulation

The main power reference signal, which is responsible of smoothing the injected real power, is generated using the linear regression analysis (*LR*). The *LR* is a statistical method that uses the running readings to predict the future trend by linearizing the relationship between time and the measured variable [14]. Hence, this method can be applied on the actual real power of WF2 to generate the fixed-slope power reference ramp to regulate the converter output power. The *LR* model to find the data at *K+1* step can be defined by:

$$P_{(k+1)} = \beta_{0,k} + \beta_{1,k}\, T_{k+1} + \varepsilon \tag{1}$$

where *P* is the predicted dependent variable (real power in this case), *T* is the corresponding time, β_0 and β_1 are the y-intercept and ramp slope, respectively, whereas ε is a random error to compensate the lost accuracy throughout the linearization process. The coefficients β_0 and β_1 can be obtained based on the least square method (LSM) since it provides a data fitting result with minimum sum of the squared distance between the actual and fitted data [12]. The LSM are defined as:

$$\beta_1 = \left[n\sum_i^k (P_x\, T_x) - \sum_i^k P_x \sum_i^k T_x\right] \Big/ \left[n\sum_i^k (T_x)^2 - \left(\sum_i^k T_x\right)^2\right] \tag{2}$$

$$\beta_0 = \left[\sum_i^k (P_x) - \beta_1 \sum_i^k (T_x)\right] \Big/ n \tag{3}$$

where *n* is the number of used data, or called window size, and equals the difference between the immediate reading subscription *k* and the initial value of the pervious data index *i*. Based on trial and error analysis through extensive simulations, window size=3 and 10 minutes step time of the regression process every 1.5 hour, yields a best fit to smooth the injected power from WF2.

On top of that, additional reference signals provided by frequency and voltage-droop (ωU-droop) controller for grid-supporting converters are used to regulate the grid frequency and voltage [15]. The frequency regulation control mode is always activated while the voltage regulation control mode is activated when switch *Sb* is in position 1 (Fig. 9). The role of ωU-droop is to adjust the active and reactive power based on power dispatch to suppress the voltage and frequency variation due to load profile changes. Based on the dynamic model of the dc-ac converter as shown in Fig. 4, and by assuming there is only an inductance impedance between the power converter and the interface AC bus (i.e, $X_{L,VSC} = \omega_0\ \{L_f + L_T\}$), therefore, the converter output real and reactive powers can be obtained by:

$$\begin{cases} P_{VSC} = \dfrac{U_c U_s}{X_{L,VSC}}\, sin(\delta - \theta) \\ Q_{VSC} = \dfrac{1}{X_{L,VSC}}\left[U_c^2 - U_c U_s\, cos(\delta - \theta)\right] \end{cases} \tag{4}$$

where δ and θ are the power and power factor angle; respectively. In case that the difference between the power and power factor angle is very small (less than 0.1 *rad*), then we can simplify the output power equations (4) to:

$$\begin{cases} P_{VSC}\, X_{L,VSC} \approx U_c U_s\, (\delta - \theta) \\ Q_{VSC}\, X_{L,VSC} \approx U_c\, [U_c - U_s] \end{cases} \tag{5}$$

As seen from (5), the active power depends on the power angle δ, while the reactive power depends only on the terminal voltage of the power converter. Therefore, the angular frequency versus real power (ω–*P*) and output voltage versus reactive power (*U*–*Q*) droop characteristics are used to regulate the grid bus frequency and voltage amplitude. In this case, the converter behaves like a power source and its controller circuit is designed based on the variation of the grid frequency and voltage with the following reference values:

$$\begin{cases} P_{\omega,ref} = P_n - P = K_p\, (\omega_n - \omega) \\ Q_{U,ref} = Q_n - Q = K_q\, \left(U_{s,n} - U_{s,n}\right) \end{cases} \tag{6}$$

where P_n and Q_n are the nominal real and reactive powers that is needed to reach the nominal voltage $U_{s,n}$ and frequency ω_n.

K_p and K_q are the proportional drooping frequency and voltage coefficient, respectively, which are corresponded to P_n and Q_n in the ω-P and U-Q droop curves as shown in Fig. 7. Lastly, to improve the THD of the injected current, the opposite phase shift of its high frequency harmonics, extracted using a high pass filter HPF, are fed to the inner loop current controller.

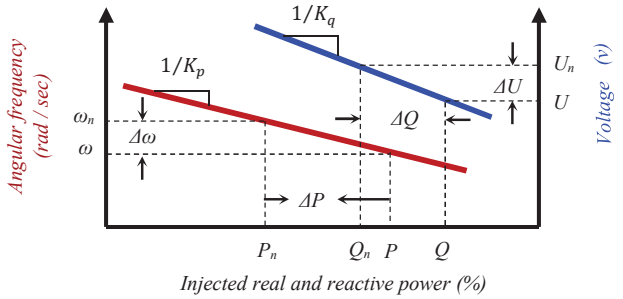

Fig. 7. ω-P, U-Q droop curves of ωU-droop controller.

Since The power factor of the injected power depends on the following expression:

$$PF = P_{inj} \Big/ \sqrt{\left(P_{inj}^{\,2} + Q_{inj}^{\,2}\right)} \tag{7}$$

$$Q_{inj} = Q_{WF2} + Q_{VSC} = U_s\,(I_s + I_{WF2})\,sin\,(\varphi) \tag{8}$$

where P_{inj} and Q_{inj} are the injected active and reactive powers. The power angle φ should tends to zero in order to reach the unity power factor. This can be done by controlling the q-axis component of the power converter current to make its summation with WF2 current in-phase with the interface bus voltage. This control mode is activated when switch *Sb* is in position 2 (in Fig. 9). Figure 8 shows the control process flow of the proposed MSDC device.

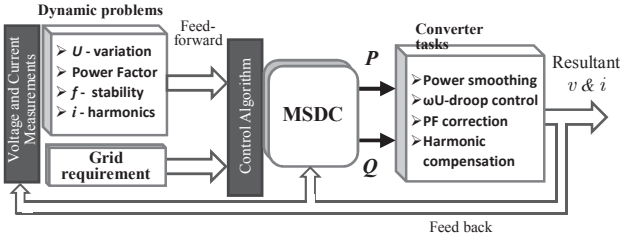

Fig. 8. Process flow of the proposed MSDC system.

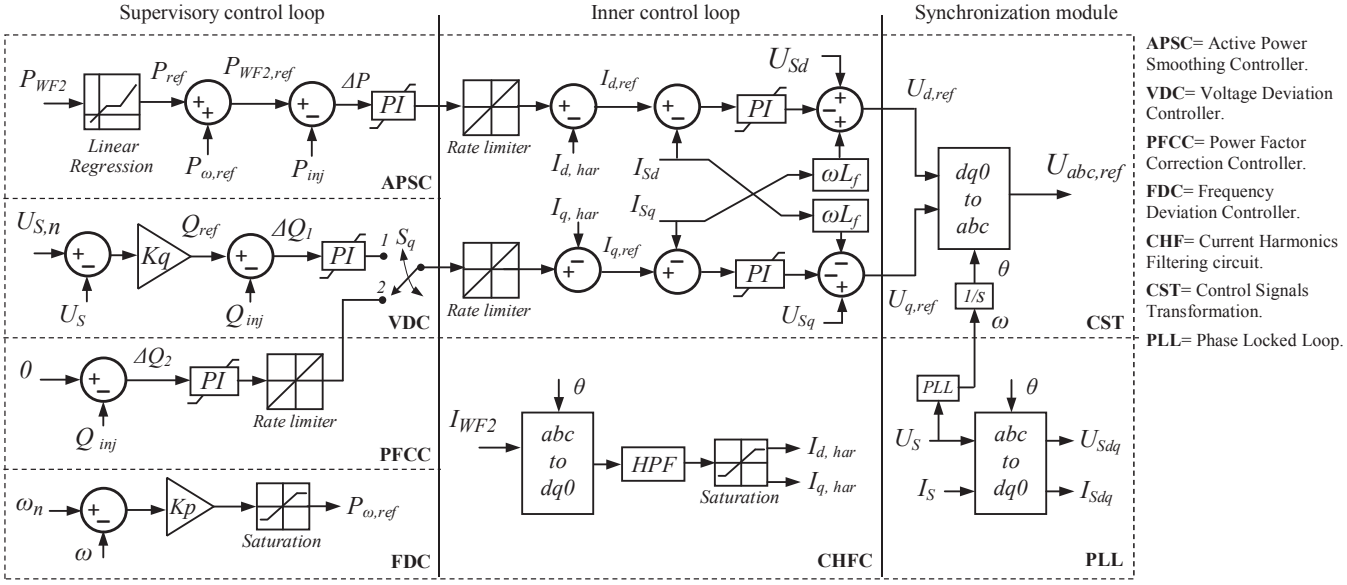

Fig. 9. Control circuit of the DC-AC converter.

B.2 Inner Control Loop Implementation

The common feedback current controller, with decoupled state variables control structure, is utilized to track the supervisory control loop reference signals by obtaining the corresponding PWM reference voltages. The decoupling process is done by substituting the converter current components, in the converter dynamic model, by the error difference between the actual and reference currents [16]. This error is fed to the proportional-integral controller (PI) of the current control circuit. The terminal voltage are also feedforwarded to the current control loop to perform the required output voltage control signals. The dynamic model of the dc-ac converter, based on the system configuration as in Fig. 4, is illustrated in (9).

$$\begin{bmatrix} U_{cd}^{\,*} \\ U_{cq}^{\,*} \end{bmatrix} = \begin{bmatrix} U_{sd} \\ U_{sq} \end{bmatrix} + \omega L_2 \begin{bmatrix} 0 & -1 \\ 1 & 0 \end{bmatrix} \begin{bmatrix} i_d \\ i_q \end{bmatrix} + K_p \begin{bmatrix} i_{d,ref} - i_d \\ i_{q,ref} - i_q \end{bmatrix} + K_i \int_0^t \begin{bmatrix} i_{d,ref} - i_d \\ i_{q,ref} - i_q \end{bmatrix} dt \tag{9}$$

The control system parameters, such as the PI controllers, are obtained through extensive simulations, with taking into account that the step-responses of the MSDC voltage and current are in a critical damped mode with minimum possible steady state error.

V. SIMULATION ANALYSIS

A. Power System Model Validation

The 12-bus power system has been developed in PSCAD/EMTDC with the same system configuration and parameters provided by BPA. A typical 48-hours operation (with 5-min sampling rate) was carefully selected to cover all possible injected power scenarios. The real data of generated powers from system synchronous generators and the two WFs (as in Fig. 10) were embedded to the simulation model.

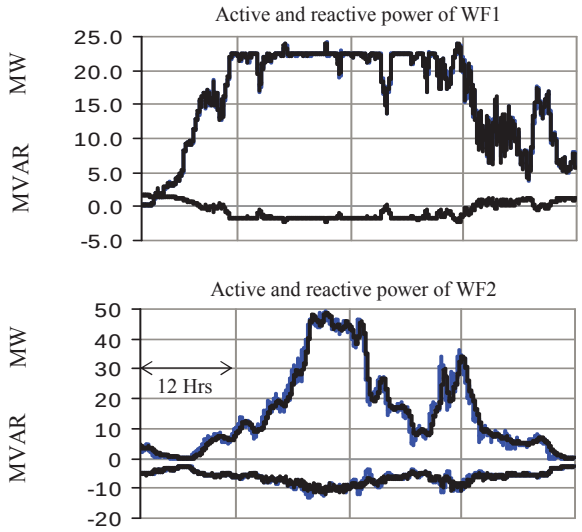

Fig. 10. Injected power form WF1 and WF2. (black) actual data and (blue) simulation results.

A comparison between selected actual data and simulation results is shown in Fig. 11. It is concluded from the illustrated results that the magnitude and fluctuation trend of real power, reactive power and voltage simulated by the developed model are match the field data quite well. Therefore, the performance of the system model in continuous operation for certain time interval was validated, and can be used in investigating the dynamic impact of the proposed MSDC device.

It is worth mentioning that the slight mismatch between filed data and simulated ones is due to some non-monitored loads and the approximation in transmission lines parameters and transformers tap-changing settings. It is clearly seen from Fig. 10 and Fig. 11 that the injected power from WF2 and voltage of bus #4 and bus #6 are aggressively fluctuating in terms of short and long time periods. In addition, the power factor of WF2 injected power is adversely affected by the uncontrolled capacitive reactive power.

B. MSDC Dynamic Response Test

The dynamic step response of the MSDC device is evaluated to validate its power control ability. For this purpose, the active and reactive powers were regulated at their maximum ratings with all possible compensations during charging and discharging modes as shown in Fig. 12. According to the results, the MSDC has the ability of controlling its output power in four operation quadrants, with maintaining the required dynamic requirements. It is worth mentioning that that dc link voltage and ESS dc currnt are changing agressively during the step change in the active or reactive powers, therefore, it is recommended to utilize a rate limiter for the power references in the contoller curcuit.

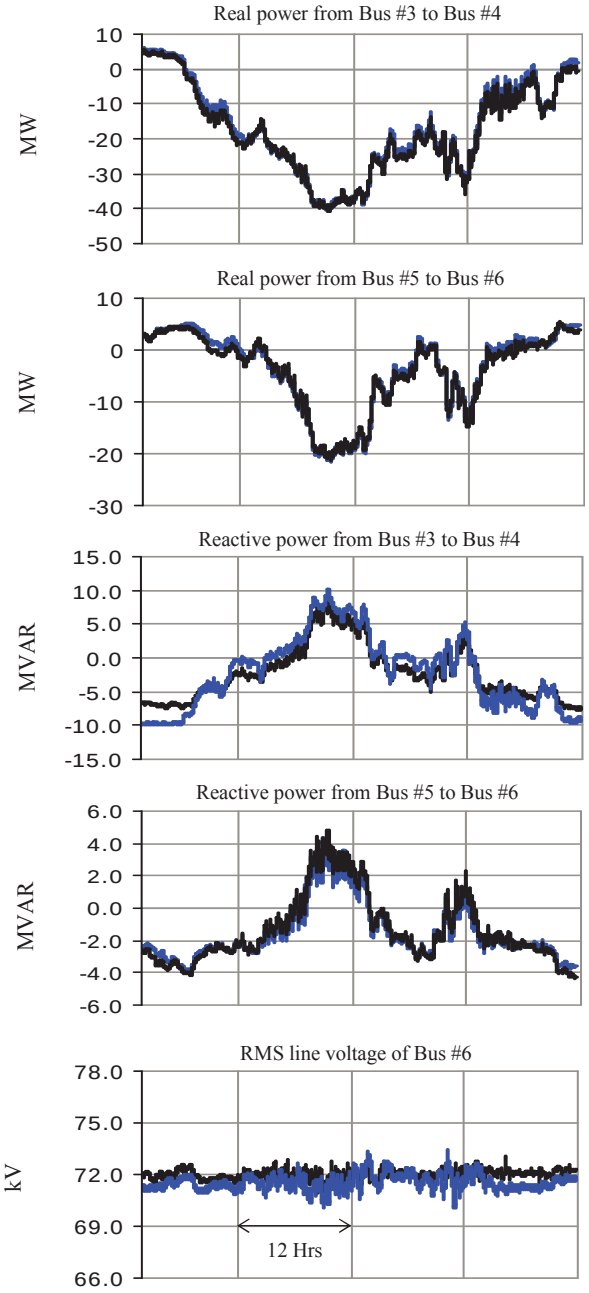

Fig. 11. Comparison of system actual data (black) and simulation model results (blue).

C. MSDC Dynamic Impact Evaluation

The dynamic impact of the MSDC, when it is connected to the power system, is demonstrated in figures 13-17. Fig. 13 shows the smoothed injected power when the MSDC output power compensates the fluctuations in the WF2 real power. This operation mode is carried out along with the PFCC mode, therefor, the MSDC works to reach zero injected reactive power

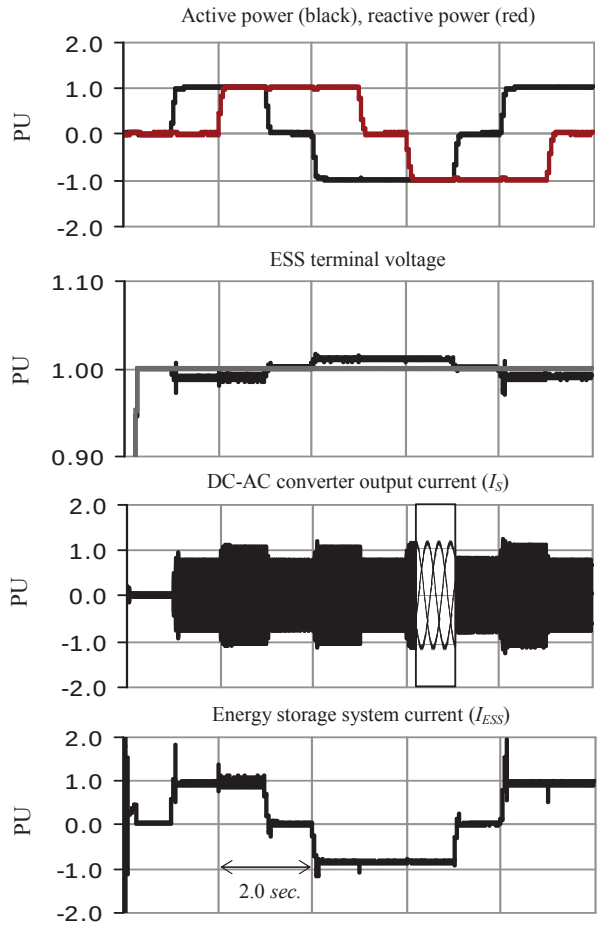

Fig. 12. Dynamic performance test of the MSDC.

and therefore unity power factor (Fig. 14). The negative power factor value means that small amount of real power is flowing from the grid to the WF2 due to power losses, whereas zero value is when there is no injected real power. The current harmonics filtering mode (CHF) is applied, after 1 hour of initial time, to suppress the harmonics in the current injected into bus #6, consequently, the voltage harmonics at bus #6 are also got suppressed as shown in Fig. 15. The harmonics contents were reduced from 5.9%, 2.2% to 2.6%, 0.57% for the POI bus voltage and current, respectively. This reduction in harmonics verifies the positive dynamic impact of the MSDC on the integration of a distorted distributed generation, due to the nature of the energy resource or the power electronic based devices integrated in the WF sub-transmission system. It is worth mentioning that the current and voltage harmonics at the POI bus with using the MSDC system, and before applying the CHF mode, are slightly higher than the harmonics during the uncontrolled POI bus operation. This slight increment in voltage and current harmonics is due to the un-sinusoidal voltage produced by the dc-ac voltage source power converter.

The MSDC device is also tested when the VDC operation mode is selected. Fig. 16 shows the dynamic enhancement of bus #6 voltage when the injected reactive power is controlled accordingly. The resultant voltage is regulated around the reference value (72.0 kV) with lower positive and negative deviations. The corresponding reactive power to regulate the POI bus voltage is also shown in Fig. 16. In this case, the MSDC device compensate for the capacitive reactive power (about 5 Mvar) with opposite oscillation of the injected reactive power.

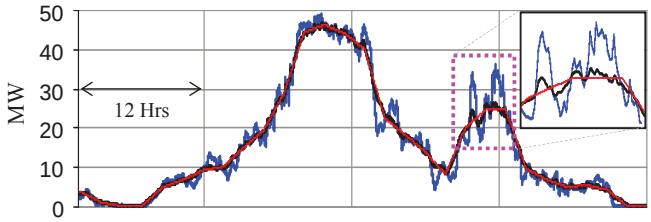

Fig. 13. Injected real power into the POI bus. (blue) with no control, (black) with using MSDC and (red) is the reference power signal.

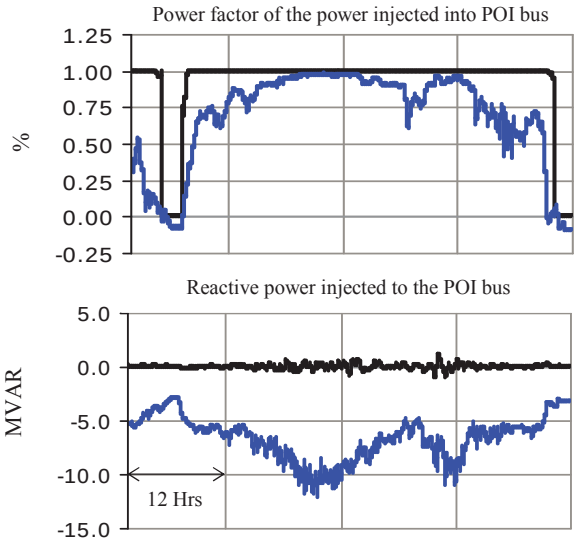

Fig. 14. Power factor and injected reactive power of bus #6 during PFCC mode. (blue) with no control and (black) with using MSDC.

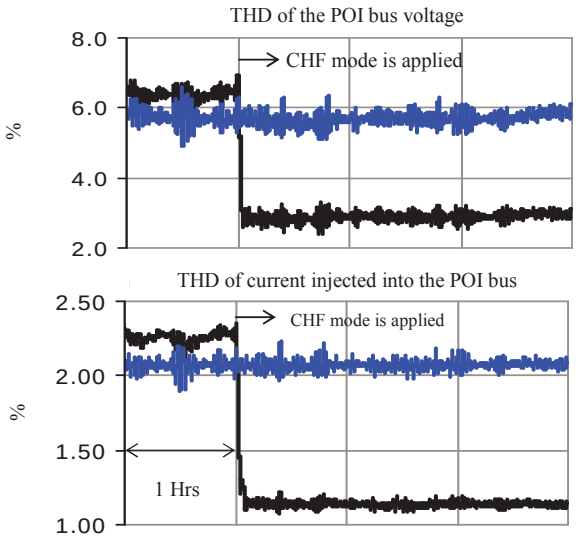

Fig. 15. THD of voltage and current at the POI bus. (blue) with no control and (black) with using MSDC.

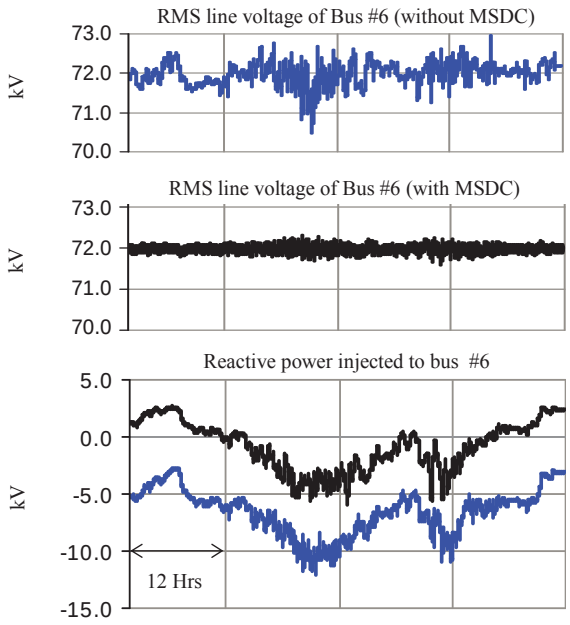

Fig. 16. Line voltage and injected reactive power of the POI bus during VDC mode. (blue) with no control and (black) with using MSDC.

The system frequency response under sudden change (±10MW) in the injected power with and without using the MSDC is evaluated as shown in Fig. 17. According to the results, the frequency nadir reduced from 0.7 Hz to 0.2 Hz.

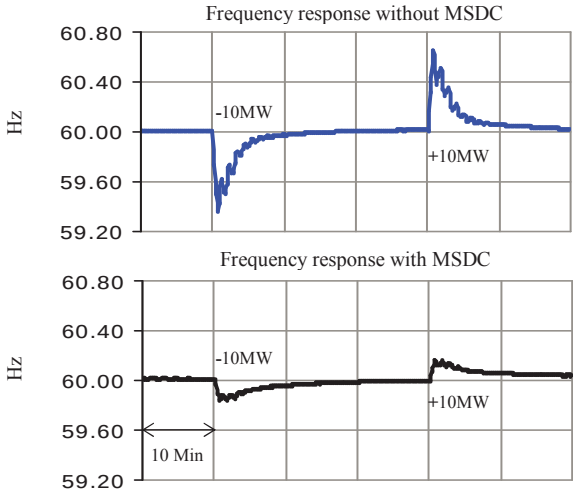

Fig. 17. Frequency response of the POI bus voltage under sudden change in the injected real power.

VI. Conclusions

This paper proposes a modular static distribution controller (MSDC), which is utilized to facilitate the integration of a large-scale wind farm (WF) into a weak power system. This device can be connected at medium voltage bus to perform several tasks in order to improve the injected power quality and dynamic performance to meet the technical specifications required in grid codes. First, an actual power system contains of two WFs is modeled and validated using the actual filed data. The power quality issues and dynamic performance problems are addressed. Second, the detailed model and control algorithms of the MSDC are developed. Third, the MSDC transient response and dynamic impacts are studied. The year-round simulation analysis, adopted by PSCAD, indicate that the proposed solution is feasible and has the ability to achieve the desired function with the size of 10MVA.

Acknowledgment

This work was supported, in part, by the National Science Foundation. We would like to thank the FREEDM CENTER, North Carolina State University, Raleigh, NC. for providing the RTDS facility. Also, we would like to thank King Saud University, Riyadh, Saudi Arabia and Saudi Arabian Cultural Mission, Fairfax, VA, 22031, for their support.

References

[1] X. Liang, "Emerging Power Quality Challenges Due to Integration of Renewable Energy Sources," in *IEEE Transactions on Industry Applications*, vol. 53, no. 2, pp. 855-866, March-April 2017.

[2] Asrari, T. Wu and S. Lotfifard, "The Impacts of Distributed Energy Sources on Distribution Network Reconfiguration," in *IEEE Transactions on Energy Conversion*, vol. 31, no. 2, pp. 606-613, 2016.

[3] Brendan Fox *and et al.*, "Wind Power Integration: Connection and System Operation Aspects." 2nd ed., London, IET, 2014.

[4] Z. H. Rather *et al.*, "Dynamic Reactive Power Compensation of Large-Scale Wind Integrated Power System," in *IEEE Transactions on Power Systems*, vol. 30, no. 5, pp. 2516-2526, Sept. 2015.

[5] M. Jafari, M. Popat and B. Wu, "Power Factor Control in a Wind Energy Conversion System via Synchronous Generator Excitation," in *Canadian Journal of Electrical and Computer Engineering*, vol. 37, no. 3, pp. 145-150, Summer 2014.

[6] N. Nguyen and J. Mitra, "Reliability of Power System with High Wind Penetration Under Frequency Stability Constraint," in *IEEE Transactions on Power Systems*, vol. 33, no. 1, pp. 985-994, Jan. 2018.

[7] M. P. Musau, T. L. Chepkania, A. N. Odero and C. W. Wekesa, "Effects of renewable energy on frequency stability: A proposed case study of the Kenyan grid," *2017 IEEE PES PowerAfrica*, Accra, 2017, pp. 12-15.

[8] International Energy Agency, market report series, renewables, Feb. 2018, URL: http://www.iea.org/

[9] X. Liang, "Emerging Power Quality Challenges Due to Integration of Renewable Energy Sources," in *IEEE Transactions on Industry Applications*, vol. 53, no. 2, pp. 855-866, March-April 2017.

[10] A. H. Bonnett, H. Glatt and S. Hauck, "Effect of Power Deviations on Squirrel-Cage Induction Motors: Addressing the Impact of Voltage and Frequency Variations," in *IEEE Industry Applications Magazine*, vol. 22, no. 6, pp. 39-47, Nov.-Dec. 2016.

[11] L. Baruschka and A. Mertens, "Comparison of Cascaded H-Bridge and Modular Multilevel Converters for BESS application," *2011 IEEE Energy Conversion Congress and Exposition*, Phoenix, AZ, 2011.

[12] Robert Sheehan, "Current-Mode Modeling for Peak, Valley and Emulated Control Methods," National Semiconductor white paper, July 31, 2007.

[13] S. K. Mazumder and K. Acharya, "Multiple Lyapunov Function Based Reaching Condition for Orbital Existence of Switching Power Converters," in *IEEE Transactions on Power Electronics*, vol. 23, no. 3, pp. 1449-1471, May 2008.

[14] X. Yan and X. Su, "Linear regression analysis. Theory and Computing." New Yok. World Scientific, 2009, pp. 201–204.

[15] A. El Moubarek *et al.*, "Simulation of droop control strategy for parallel inverters in autonomous AC microgrids," *2016 8th (ICMIC)*, Algiers, 2016.

[16] Amirnaser Yazdani and Reza Iravani, "Voltage-Sourced Converters in Power Systems: Modeling, Control, and Applications," John Wiley and Sons, Inc., Hoboken, New Jersey. IEEE Press, 2010.